The β1-integrin-dependent function of RECK in physiologic and tumor angiogenesis

Revised version of MCR-09-0351R

The β1-integrin-dependent function of RECK in physiological and tumor angiogenesis

Takao Miki [1,2,3], Awad Shamma [1,2], Shunsuke Kitajima [1], Yujiro Takegami [1], Makoto Noda [1], Yasuaki Nakashima [4], Ken-ichiro Watanabe [5] and Chiaki Takahashi [1,2,6]

[1] Department of Molecular Oncology, Kyoto University Graduate School of Medicine, Yoshida-Konoe-cho, Sakyo-ku, Kyoto 606-8501, Japan

[2] The 21st Century Center of Excellence Program, Kyoto University Graduate School of Medicine, Yoshida-Konoe-cho, Sakyo-ku, Kyoto 606-8501, Japan

[3] Department of Biochemistry and Molecular Biology, University of Texas Health Science Center-Houston, Houston, Texas 77030, USA

[4] Laboratory of Anatomic Pathology, Kyoto University Hospital, 54 Shogoin-Kawahara-cho, Sakyo-ku, Kyoto 606-8507, Japan

[5] Department of Pediatrics, Kyoto University Hospital, 54 Shogoin-Kawahara-cho, Sakyo-ku, Kyoto 606-8507, Japan

[6] Division of Oncology and Molecular Biology, Center for Cancer and Stem Cell Research, Cancer Research Institute, Kanazawa University, Kakuma-cho, Kanazawa 920-1192, Japan

Running title: Tumor-promoting function of vascular RECK

Correspondence: Chiaki Takahashi MD., PhD., Professor, Division of Oncology and Molecular Biology, Center for Cancer and Stem Cell Research, Cancer Research Institute, Kanazawa University, Kakuma-cho, Kanazawa 920-1192, Japan. Tel: +81-76-264-6750, Fax: +81-76-234-4521, e-mail: chtakaha@staff.kanazawa-u.ac.jp

Abstract

Vascular endothelial cells produce considerable amounts of matrix metalloproteinases (MMPs), including MMP-2, MMP-9 and membrane type 1 (MT1)-MMP. However, little is known about the regulatory mechanisms of these protease activities exhibited during vascular development. A glycosylphosphatidylinositol (GPI)-anchored glycoprotein, reversion-inducing cysteine-rich protein with Kazal motifs (RECK), has been shown to attenuate MMP-2 maturation by directly interacting with MT1-MMP. Here, we show that an angiogenic factor angiopoietin-1 induces RECK expression in human umbilical vein endothelial cells (HUVECs), and RECK depletion in these cells results in defective vascular tube formation and cellular senescence. We further observed that RECK depletion downregulates β1-integrin activation, which was associated with decreased autophosphorylation of focal adhesion kinase (FAK) and increased expression of a cyclin-dependent kinase (CDK) inhibitor $p21^{CIP1}$. In agreement, significant downregulation of β1-integrin activity was observed in vascular endothelial cells in *Reck*-/- mouse embryos. In HUVECs, specific inhibition of MMP-2 significantly antagonized

the effect of RECK depletion on β1-integrin signaling, cell proliferation and tube elongation. Furthermore, we observed that hyper-vascular tumor-derived cell lines can induce high RECK expression in convoluted vascular endothelial cells, and this in turn supports tumor growth. Targeting RECK specifically in tumor-associated vascular endothelial cells resulted in tumor regression. Therefore, we propose that RECK in tumor vascular endothelial cells can be an interesting target of cancer treatment via abortion of tumor angiogenesis.

Introduction

MMPs are Ca^{++} and Zn^{++}-dependent endopeptidases that play crucial roles in the degradation of various extracellular matrix (ECM) components (1). In addition, recent studies have demonstrated that these enzymes exert unique biological functions by acting on various important modulators of cellular functions (2,3). During tumor propagation, not only tumor cells but also stromal cells, including vascular endothelial cells, produce considerable amounts of MMPs (4). In particular, during angiogenesis engaged by endothelial cells, MMPs play both positive and negative roles (5). The pro-angiogenic functions of MMPs include degradation of ECM components, which facilitates the invasion and migration of endothelial cells, cleavage of endothelial cell-cell adhesion mediated by cadherins, generation of cryptic integrin-binding sites from ECM components, and enhancement of the bioavailability of various growth factors such as vascular endothelial growth factor (VEGF), transforming growth factor β (TGFβ) and

connective tissue growth factor (CTGF) (5). On the other hand, the anti-angiogenic functions of MMPs include ectodomain shedding of receptors for growth factors such as fibroblast growth factor receptor 1 (FGFR1) and urokinase-type plasminogen activator receptor (uPAR), resulting in the inhibition of growth signals generated from these receptors (5). Other anti-angiogenic functions of MMPs include generation of cryptic angiogenesis inhibitors from plasminogen or collagens, such as angiostatin, endostatin, tumstatin, arrestin or canstatin; all of these are supposed to exert their anti-angiogenic functions by interacting with various forms of integrins including $\alpha5\beta1$, $\alpha v\beta3$, $\alpha1\beta1$ and $\alpha3\beta1$ (5,6). Moreover, soluble hemopexin (PEX) domain derived from degraded MMP-2 blocks the binding of intact MMP-2 to integrin $\alpha v\beta3$ (7). These findings suggest that the anti-angiogenic functions of MMPs profoundly involve integrin signaling.

Integrins principally serve as adhesion receptors for ECM components and provide the central system to transduce biochemical signals from outside of the cells (6). Ligand occupancy and the resultant clustering of integrin receptors induce autophosphorylation of FAK, which evokes cellular actions (proliferation, migration, spreading or apoptosis) that enable cells to adjust to changes in the extracellular environment (8).

The *RECK* gene has been identified as a negative transcriptional target of molecules, including multiple retroviral oncogenes (9), Epstein-Barr virus latent membrane protein 1 (LMP1) (10), histone deacetylase (HDAC) (11) and oncogenic micro-RNA miR-21 (12~14). The product of this gene can directly bind to a series of metalloendopeptidases, including MMP-9 (9), MMP-2 (15), MT1-MMP, CD13/APN (16) and ADAM10 (17),

and attenuate their proteolytic activity competitively in most of cases. Two metalloprotease-substrate-like domains recently discovered in RECK may provide a structural basis for its biochemical actions (Takegami and Takahashi, in preparation for publication). Yet, the most discrete structural feature of RECK compared to known primary tissue metalloprotease inhibitors, such as tissue inhibitors of metalloproteinases (TIMPs) and α2-macroglobulins (18), is that RECK is covalently anchored to the plasma membrane surface via glycosylphosphatidylinositol (GPI)-anchors. Because of this structural feature, RECK controls metalloendopeptidase activities in highly limited distance from the membrane surface (perimembrane area), and moreover, it exerts unique functions by interacting with membrane-tethered metalloendopeptidases. Indeed, molecular interaction between RECK and MT1-MMP enables MT1-MMP to translocate to the lipid raft fraction, which consequently changes the route of MT1-MMP endocytosis to one that is specific to that of GPI-anchored proteins; this results in a shorter half life of MT1-MMP (16). Furthermore, RECK was found to stabilize the interaction between membrane-bound Notch ligands and Notch receptors by protecting Notch ligands from ADAM10-mediated ectodomain shedding, which critically contributes to the maintenance of the self-renewal property of neural stem cells (17).

We recently observed that treatment with an angiogenic factor, namely, angiopoietin-1, or coculture with hyper-vascular tumor-derived cells markedly induced RECK expression in human umbilical vein endothelial cells (HUVECs), which indicates that RECK may possess pro-angiogenic function. Indeed, severe developmental defects in the vascular network were observed in the previous analysis of *Reck*$^{-/-}$ embryos (15). No such vascular

phenotypes were observed in mice deficient in known soluble MMP inhibitors (18). We further examined *Reck*-/- mice, and identified significant developmental defects in vascular endothelial cells. Although the vascular phenotype appearing in *Reck*$^{-/-}$ embryos can be attributed not only to the defects in endothelial cells but also to those in smooth muscle cells, pericytes and the surrounding stromal cells, in this study, we focused on the role of RECK in the development of vascular endothelial cells under physiological and pathological (tumor angiogenesis) conditions mainly by employing RNA interference techniques.

Materials and Methods

Cell culture and transfection. The human umbilical vein endothelial cells (HUVECs; CC2517, CAMBREX) were maintained in EBM-2 (growth factor-free) or EGM-2 (supplemented with endothelial cell growth factors) bullet kit (CC-3162, CAMBREX) and used between passage 3 to 6. Tumor cells were cultured in DMEM supplemented with 10% FCS. Transfection of HT1080 cells was described (16).

Antibody. The following mouse or rat primary antibodies were used: anti-RECK (9), anti-α-tubulin (CP06, Calbiochem), anti-MMP-2 (F-68, Biotechnology Products), anti-BrdU (MAB4072, Chemicon), anti-active β1-integrin (9EG7, Chemicon), anti-β1-integrin (610467, BD), anti-phosphorylated FAK (FAK^{pY397}) (611722, BD), anti-FAK (sc-557, Santa Cruz), anti-p21 (556430, BD), anti-CD31 (01951A, Pharmingen) (for nude mouse assay), anti-CD31 (ab28364, Abcam) (for human tumor), and anti-human

CD34 (hCD34) (CBL496, Chemicon) antibodies. As secondary antibodies, we used anti-mouse IgG PE (550083, BD), anti-mouse IgG Alexa fluor 555 (A21424, Molecular Probes), anti-rat IgG APC (734820, Cell Lab), anti-mouse IgG Texas red (T862, Molecular Probes) and anti-rabbit IgG Alexa fluor 488 (Molecular Probes, A11034) antibodies. For stimulating β1-integrin activation, we used mouse anti-β1 integrin monoclonal antibody (P4G11, Chemicon)(19).

Immunoblotting. Immunoblotting was performed as described previously (16).

Mice. *Reck*$^{+/-}$ mice (15) were crossed with C57BL/6 Cr Slc TgN(act-EGFP)OsbC14-Y01-FM131 (20), and resultant progenies were intercrossed to generate *Reck*$^{-/-}$ embryos transmitting enhanced green fluorescent protein (EGFP) gene.

RNA interference. The siRNAs specifically targeting human RECK (siRNA1: 29149; siRNA2: 29155) and EGFP (4626), and negative control (4611G) were purchased from Ambion, and those targeting MMP-2 were purchased from Invitrogen (siRNA1: 1178208, siRNA2: 1178210). 1 x 10^5 HUVECs were transfected with 50 μM siRNA using Lipofectamine2000 (Invitrogen).

MMP assay. The synthetic peptide Mca-Lys-Pro-Leu-Gly-DPA-Ala-Arg-NH_2 (5 μM) was mixed with culture supernatants from HUVECs transfected with siRNA, and incubated at 37°C for 30 min. Cleavage was measured as described previously (16). For the detection of MMP-2, culture supernatant was filtered through 0.45 μm ultrafiltration membrane

and incubated with gelatin sepharose 4B (GE healthcare) at 4 ^{o}C. Proteins bound to the beads were analyzed by immunoblotting using antibody to MMP-2. Signal intensity was measured using LAS3000 chemiluminescence imaging system (Fuji, Japan).

2D and 3D vascular formation assay. For 2D culture, 4 x 10^4 HUVECs transduced with siRNA were grown on growth factor-reduced Matrigel (354230, BD)-coated wells and incubated at 37 °C for 48 h. For 3D culture, type I collagen (Cellmatrix type I-A, Nitta gelatin) solution was mixed on ice with 10 x Modified Eagle's Medium, and then with 1 x 10^6 cells/ml. The mixture was allowed to solidify for 30 min at 37°C, and incubated with EGM-2 bullet kit supplemented with 50 ng/ml phorbol 12-myristate 13-acetate (PMA) for 5 days.

RT-PCR. RNA was extracted using Trizol (15596-026, Invitrogen) and reverse transcribed using TaKaRa RNA PCR kit (RR019A, TaKaRa). PCR was performed with specific primer sets: RECK (30 cycles), sense: 5'-ACTCCCTCCTCCTTCCCCTCAGC-3'; antisense: 5'-ATTTAATCAGCTTGCTTTTGCAT-3', GAPDH (28 cycles), sense: 5'-ACCACAGTCCATGCCATCAC-3'; antisense: 5'-TCCACCACCCTGTTGCTGTA-3', β1-integrin, sense: 5'-TTATCCTTCTATTGCTCACCTTGTC-3'; antisense: 5'-ATAACCTCTACTTCCTCCGTAAAGC-3'.

Proliferation assay. HUVECs were grown on 96-well type plates (2 x 10^3 cells/well). After siRNA transfection, the cell numbers were subsequently quantified using Cell Count reagent SF (07553-15, Nacalai tesque, Japan).

BrdU uptake and cell cycle. Cultured cells were incubated with 3 μg/ml of 5-bromo-2'-deoxyuridine (BrdU) for 90 min, trypsinized, and fixed with 70% ethanol. E9.5 embryos were labeled *in utero* for 2 h by a single pulse of BrdU (3 mg). Samples were reacted with anti-BrdU and then with anti-mouse IgG PE antibody, and subjected to flow cytometry-assisted cell sorting (FACS) analysis. For measuring propidium iodide (PI) incorporation, cells were fixed with 4% paraformadldehyde (PFA) in phosphate buffered saline (PBS) and suspended in PBS with 50 μg/mL PI and 100 U/mL Ribonuclease A. At least 10,000 events were acquired,

SA-β gal assay. Senescence-associated (SA)-β galactosidase (β-gal) activity in cells was detected as described previously (21).

FACS analysis. HUVECs were trypsinized, fixed with 4% PFA, suspended in PBS with 0.5% bovine serum albumin (BSA), and stained with anti-β1-integrin antibodies (active form: 9EG7; total β1 integrin: P4G11) and secondary with anti-rat IgG-APC or anti-mouse IgG-PE, respectively. Data were collected using FACS Aria (BD Biosciences).

Immunohistochemistry. The specimens were fixed with 1% PFA, embedded in optimal cutting temperature (OCT) compound, and stained as described previously (17).

Luciferase assay. 4 x 10^5 HUVECs were plated onto 60 mm dishes, and transfected with mouse *Reck* promoter luciferase reporter pGL3-4110-luc (22) and pCMV-β-gal

expression vector (21). Twenty-four hours after transfection, cells were trypsinized, mixed with 4 x 10^5 tumor cells, and cultured for 24 h. Luciferase and β-gal activities in cells were measured as described (23). β-gal activity was used to normalize luciferase activity in each transfection.

Human tumors. Biopsy samples of adrenal mass were collected from two patients with neuroblastoma who had been treated at Kyoto University Hospital, and analyzed according to the guideline of Kyoto University Graduate School of Medicine. Informed consent was obtained from the guardians of patients.

SCID mouse model of tumor angiogenesis. Porous poly-L-lactic acid (PLLA) (Sigma) scaffolds were prepared as described (24). 5 x 10^5 siRNA-transfected HUVECs and HT1080 cells each were mixed with Matrigel, loaded into scaffolds, and implanted subcutaneously into five-week-old female severe combined immunodeficiency (SCID) mice (CLEA, Osaka, JAPAN). Three weeks after transplantation, recovered scaffolds were weighed, fixed with 1% PFA in PBS, and embedded in OCT compound.

Results

Angiopoietin-1 upregulates RECK in vascular endothelial cells. To address whether RECK is involved in the development of vascular endothelial cells, we first examined the effects of various angiogenic factors on the transcriptional regulation of RECK in HUVECs cultured in EBM-2 (growth factor-free culture medium). This study revealed

that RECK expression in HUVECs was induced by angiopoietin-1, but not by vascular endothelial growth factor (VEGF), fibroblast growth factor (FGF) or epidermal growth factor (EGF) (Fig. 1A), suggesting that RECK expression is regulated in vascular endothelial cells by a specific angiogenic factor.

Abnormal vascular endothelial development in *Reck*-null embryos. A previous study revealed that *Reck*$^{-/-}$ embryos exhibited abnormal branching of vasculatures, and overexpression of RECK in tumor cells modified tumor angiogenesis (15). We therefore speculated that RECK could be implicated in both physiological and pathological angiogenesis. Additional introduction of the genetic background carrying enhanced green fluorescent protein (EGFP) transgene into *Reck*$^{-/-}$ embryos enabled us to observe the presence of significant developmental defects in vascular endothelial cells, namely, abnormal alignment and detachment from the subendothelial layer (Fig. 1B); these were not aware in the previous study without introducing EGFP background (15). We observed such obvious morphological disorders of vascular alignment in 4 out of 5 *Reck*$^{-/-}$; *EGFP* E10.0 embryos by carefully observing vasculatures in multiple slices of thin paraffin sections under fluorescence microscope, but never in 5 control embryos. These findings prompted us to examine the function of RECK specifically in vascular endothelial cells.

RECK depletion affects tube formation by HUVECs. To directly assess the role of RECK in angiogenesis, we performed siRNA-directed depletion of RECK in HUVECs cultured in EGM-2 (culture medium supplemented with growth factors), which resulted in more than 95% reduction in RECK expression at 48 h after transduction (Fig. 1C, left).

This treatment increased the net metalloendopeptidase activity detected in the culture supernatant by 2~3 fold compared to that in control supernatant (Fig. 1C, middle). We also observed increased level of active form MMP-2 in RECK-depleted HUVECs (Fig. 1C, right). HUVECs transduced with control siRNA expressed *RECK* at 6 h after plating onto Matrigel, and the cells were able to form tube-like structures and branches within 48 h. However, in HUVECs transduced with siRNA targeting RECK (Fig. 1D, top), the tubes formed under the same conditions were significantly shorter and often disconnected (Fig. 1D bottom). Shorter tube formation induced by RECK depletion was evident in type I collagen 3D gel as well as in the 2D assay (Fig. S1A, B). These findings suggest that RECK plays a critical role in physiological angiogenesis.

RECK depletion induces growth arrest and cellular senescence in HUVECs. To further characterize the primary effect of RECK depletion in HUVECs, we analyzed monolayer cells grown on non-coated plastic dish with EGM-2. HUVECs transduced with RECK siRNAs proliferated significantly slower than those transduced with control or EGFP siRNA (Fig. 2A). The G0-G1 population in cells transduced with control siRNA was 69%, and this figure increased to 85% when the cells were transduced with RECK siRNA (Fig. 2B). Similarly, bromodeoxyuridine (BrdU) incorporation was significantly reduced by RECK depletion (Fig. 2C). Twelve days after transduction of RECK siRNA, we observed a significant level of senescence-associated β-galactosidase (SA-β-gal) activity (Fig. 2D) without any evidence of increased cell death as assessed by the terminal deoxyribonucleotidyl transferase (TdT)-mediated biotin-16-dUTP nick-end labeling (TUNEL) assay (data not shown). These findings suggest that RECK critically

supports the proliferation of HUVECs.

Effects of RECK depletion on HUVECs partially depends on MMP-2. Since it was previously demonstrated that RECK inhibits the proteolytic activity of a series of metalloendopeptidases, including MMP-9 (9), MMP-2 (15), MT1-MMP, CD13/aminopeptidase N (APN) (16) and ADAM10 (17), we hypothesized that deregulated activation of any of these enzymes induced by RECK depletion would contribute to the appearance of phenotypes in HUVECs. siRNAs targeting individual genes encoding these enzymes were simultaneously introduced with RECK siRNAs into monolayer HUVECs cultured with EGM-2 (Fig. 3A and data not shown). Among tested siRNAs, MMP-2 siRNAs significantly antagonized the effect of RECK siRNAs on the proliferation of HUVECs (Fig. 3B). In contrast, depletion of MMP-2 without RECK depletion did not produce detectable impact on cell proliferation (Figure 3B), suggesting that MMP-2 acquires a specific role in the absence of RECK. In the 2D assay, the effect of RECK siRNA on tube elongation was significantly rescued by simultaneous inhibition of MMP-2 (Fig. 3C), however, the defect in tube branching was not rescued (Fig. 3D). The 3D assay results were consistent with the 2D results (Fig. S2). These findings suggest that the effects of RECK depletion on vascular formation by HUVECs partially depends on MMP-2 and that shorter tube formation correlates with proliferation defect. Furthermore, MT1-MMP nor MMP-9 depletion failed to reverse proliferation defects in RECK-depleted HUVECs (data not shown); the implication of these findings will be discussed later (see below).

RECK depletion downregulates the activation of β1-integrin and FAK in an MMP-2-dependent manner. Next, we addressed whether the involvement of MMP-2 can explain why RECK depletion suppresses the proliferation of HUVECs. Since integrins are frequent target of anti-angiogenic MMP activities (5), we measured the activity of various types of integrins using antibodies that specifically recognize the activated forms of integrins by fluorescence-activated cell sorting (FACS). This study revealed that the activation of β1-integrin is specifically affected by RECK depletion (Fig. 4A). No quantitative differences were detected between cells transduced with RECK siRNA and the controls by both FACS and immunoblotting (IB) with antibody reacting with all forms of β1-integrin (Fig. S3A). In addition, RECK depletion did not affect β1-integrin mRNA expression as assessed by reverse transcription-polymerase chain reaction (RT-PCR) (Fig. S3B). Furthermore, overexpression of RECK in HT1080 fibrosarcoma cells resulted in increased β1-integrin activation (1.7 fold induction) (Fig. 4B) without detectable alteration in the total β1-integrin expression level (Fig. S3C, D). These findings suggest that RECK stimulates β1-integrin activation in both normal and tumor cells.

To determine whether downregulation of β1-integrin activation in HUVECs induced by RECK depletion depends on MMP-2, siRNA specifically targeting MMP-2 was simultaneously introduced into these cells cultured in EGM-2. This experiment demonstrated that the simultaneous inhibition of MMP-2 activity significantly antagonizes the effect of RECK depletion on β1-integrin activation in HUVECs (Fig. 4C).

To validate the relationship between RECK and integrin signaling, we measured the autophosphorylation status of FAK as one of common downstream targets of integrin signaling (8). RECK depletion downregulated FAK phosphorylation, and this downregulation was significantly antagonized by the simultaneous depletion of MMP-2 (Fig. 4D).

RECK depletion upregulates $p21^{CIP1}$ expression in a β1-integrin-dependent manner. To prove that downregulation of β1-integrin signaling is responsible for the growth arrest and cellular senescence induced by RECK depletion in HUVECs, we treated RECK-depleted HUVECs with monoclonal antibody that was engineered to specifically stimulate β1-integrin activation (19). This experiment resulted in the significant and dose-dependent recovery of cell proliferation in RECK-depleted HUVECs in EGM-2 (Fig. 4E). Further, we observed specific induction of a CDK inhibitor $p21^{CIP1}$ in HUVECs when transduced with RECK siRNA; this effect of RECK siRNA was antagonized by treatment with the β1-integrin-stimulating monoclonal antibody (Fig. 4F). In addition, simultaneous depletion of MMP-2 antagonized the effect of RECK depletion on $p21^{CIP1}$ induction (Fig. 4G). These findings suggest that RECK stimulates FAK activation and suppresses $p21^{CIP1}$ expression by regulating β1-integrin activation in an MMP-2 dependent manner. Since FAK has been linked to Skp2-independent control of the cellular $p21^{CIP1}$ level (25), we speculated that RECK depletion induces $p21^{CIP1}$ expression by downregulation of β1-integrin signaling followed by inactivation of FAK.

***Reck*-deficiency downregulates β1-integrin activation *in vivo*.** We next examined the

activation status of β1-integrin in vascular endothelial cells in *Reck*$^{-/-}$ mice to determine the relevance of our *in vitro* findings *in vivo*. Most of *Reck*$^{-/-}$ embryos survive up to embryonic day (E)10.5 and then die abruptly due to acute hemorrhage in the abdominal vessels (15). In E10.0 wild-type embryos, CD31^{+} vascular endothelial cells abundantly express both RECK and β1-integrin. Most CD31^{+} cells express active β1-integrin in wild-type E10.0 embryos; however, in abdominal hemorrhage-free and heart beat-positive (alive) *Reck*$^{-/-}$ E10.0 embryos, we detected active β1-integrin signals with significantly less frequency although the total β1-integrin signals were at level similar to that of the wild-type (Fig 5A, B). These findings suggest that *Reck*-deficiency downregulated β1-integrin activation in the vascular endothelial cells of E10.0 mouse embryos.

Hyper-vascular tumor cells induce RECK expression in vascular endothelial cells. To investigate the role of RECK in pathological angiogenesis, we observed RECK expression in mouse-derived $CD31^+$ endothelial cells convoluted in human-derived tumor cells (HT1080) that were subcutaneously inoculated into nude mice and grown for 14 d. We observed a marked induction of RECK in mouse-derived $CD31^+$ cells in the tumors (Fig. 6A). This phenomenon was recapitulated *in vitro* by co-culturing HUVECs with tumor cells on a non-coated dish. Significant induction of RECK under this condition was confirmed by IB and the reporter assay for the *Reck* promoter (Fig. 6B top and S4A). Hypoxic condition did not induce RECK expression in HUVECs (data not shown); thus, we speculated that tumor cells directly induce the transcription of RECK in vascular endothelial cells convoluted in the tumor mass.

A comparison of the RECK-inducing activity exerted by various human tumor-derived cell lines revealed that RECK-induction well correlates with the known angiogenic activity of each cell line; cell lines derived from hyper-vascular tumors (HT1080: fibrosarcoma; SKNSH: neuroblastoma; PC-12: pheochromocytoma) tend to induce higher RECK expression in cocultured HUVECs (Fig. 6B, bottom). Moreover, 2 out of these 3 tumor cell lines induced a significant level of *Reck* promoter activation in coclutured HUVECs (Fig. S4), suggesting that RECK-induction by tumor cells is at least partially dependent on transcriptional control. MCF-7 was exceptional; this line significantly transactivated RECK promoter reporter (Fig. 4B), however, only slightly upregulated RECK protein expression (Fig. 6B). Interestingly, cell lines with higher RECK-inducing activity also tend to express a detectable level of endogenous RECK (Fig.

6B bottom), implicating that RECK could be induced in such tumors by an autocrine mechanism. However, depletion of endogenously expressed RECK in one of these RECK-positive tumor cell lines (HT1080) did not result in detectable changes in cell behavior including proliferation, cell death, migration and invasion (data not shown).

To examine the clinical relevance of RECK induction in vascular endothelial cells convoluted in tumors in nude mice, we analyzed tumor biopsy tissues from human neuroblastomas. As described, these tumors exhibited a high density of vasculature (Fig 6C, top). We observed weak but significant level of RECK expression in $CD31^+$ vascular endothelial cells found within the tumor mass (Fig. 6C, bottom). Similarly, the endothelial cells of the larger arteries located close to the tumor mass showed significant level of RECK expression. In these arteries, smooth muscle cells also express RECK as described previously (15)(Fig. S5). Although not directly addressing whether RECK is induced during neuroblastoma development, this study shows that vascular endothelial cells at least in human neuroblastomas express a detectable level of RECK.

RECK induction is required for vascular endothelial cells to support tumor growth. To determine the biological significance of RECK induction in vascular endothelial cells by tumor cells, we employed a tumor angiogenesis model in which human endothelial cells (HUVECs) and human fibrosarcoma cells (HT1080) were mixed with Matrigel, and allowed to adhere to porous poly-L-lactic acid (PLLA) scaffolds. The complex was subcutaneously implanted into SCID mice, and grown for 3 weeks.

To distinguish HUVECs from host mouse-derived vascular endothelial cells, we used an antibody that specifically reacts with human CD34 (hCD34). HUVECs ($CD31^+/hCD34^+$) were detected more frequently at the center of the tumors than in the marginal areas (Fig. 6D, top). The marginal areas were frequently occupied by host mouse-derived $CD31^+/hCD34^-$ cells (Fig. 6D, top). The complex containing HUVECs transduced with RECK siRNA produced significantly smaller tumors compared to the controls (Fig. 6D, right). Histological analysis revealed a poorer vasculature and a higher degree of necrosis at the center of tumors containing HUVECs transduced with RECK siRNA than those in the case of tumors containing HUVECs transduced with control siRNA (Fig. 6D, bottom and right). These findings suggest that RECK induction in vascular endothelial cells by tumor cells is required for supporting tumor growth.

Discussion

In this study, we demonstrated that RECK is induced in vascular endothelial cells by a specific angiogenic factor during physiological angiogenesis, and in hyper-vascular tumors during pathological angiogenesis. In addition, we characterized the pro-angiogenic function of RECK, which appeared to at least partially depend on MMP-2 and β1-integrin. A similar functional interaction between MMP-2 and β1-integrin signaling has been reported in previous analyses of cardiac myocytes (26) and chondrogenic cells (27). Thus far, no evidence of a direct interaction between MMP-2 and β1-integrin is available. Therefore, we currently speculate that when RECK expression is attenuated in vascular endothelial cells, substrates of MMP-2 may participate in the negative regulation

of β1-integrin activation as suggested previously (26, 27).

However, in the current study, it was not clarified why simultaneous MMP-2 depletion specifically antagonized the effects of RECK depletion on proliferation of HUVECs. It was reported that a selective MT1-MMP inhibitor almost completely blocked proMMP-2 processing in HUVECs (28). However, MT1-MMP depletion was not relevant to MMP-2 depletion in RECK-depleted HUVECs in our experiment. Since proMMP-2 is not the sole substrate of MT1-MMP (29), we speculate that MT1-MMP can exert distinct pro- and anti-angiogenic functions even in an MMP-2-independent manner. Thus, we further speculate that suppression of the MMP-2-indepdent pro-angiogenic (growth-stimulating) function of MT1-MMP masked the rescue effect of MT1-MMP depletion on RECK-depletion-induced proliferation defects. MMP-9 depletion may have failed to rescue rescue the RECK-depletion-induced proliferation defects due to similar reason. Overall, these findings indicate bivalent roles of MMP activities in angiogenesis.

Another new insight provided by this study is that proliferation of vascular endothelial cells during physiological and pathological angiogenesis is critically controlled by RECK. As discussed above, MMP activities provided by vascular endothelial cells can be both pro- and anti-angiogenic to the cells themselves. RECK may function to protect proliferating vascular endothelial cells from self-produced anti-angiogenic MMP activities, as well as from those generated by tumor stromal cells or tumor cells. Specific downregulation of RECK in vascular endothelial cells decreased their contribution to tumor growth. Conversely, RECK overexpression in experimentally transplanted tumor

cells reduced tumor volume by attenuating angiogenesis from host nude mice (15). These findings suggest that the effect of RECK on tumor angiogenesis varies depending on the location of expression.

RECK expression was undetectable in most of commonly available tumor cell lines by conventional IB techniques (9). By applying highly sensitive IB methods, we established that PC-12 and HT1080 show the highest endogenous RECK expression among the tumor cell lines; however, the level of RECK expressed in these cell lines is far less than that in proliferating vascular endothelial cells. In addition, depletion of endogenous RECK in HT1080 cells did not show detectable changes in cell behavior. Thus, we propose the possibility that RECK principally functions in vascular endothelial cells rather than in tumor cells, and supports tumor growth by enhancing angiogenesis rather than suppressing it. This statement seems to be contradictory to studies showing positive correlation between RECK expression level in tumor tissues and favorable prognosis of cancer patients (30, 31). However, virtually none of such studies discriminated RECK expression in tumor cells, stromal cells, tumor vessels or other cell lineages composing tumors. Furthermore, we still do not know whether RECK actively improves prognosis, or the elevated RECK expression is a consequence of less malignant property of tumor cells. We recently obtained evidence that RECK promotes self-renewing activity of neural stem cells through modulation of Notch signaling (17), and, inversely, suppresses proliferation of colorectal cancer cells and mouse embryonic fibroblasts through another cellular signaling pathway (Kitajima et al, unpublished). These findings indicate that as MMPs are multi-functional, RECK is multi-functional and bivalent especially in growth

control.

Finally, this study proposed that tumor cells may actively induce RECK expression in the surrounding vascular endothelial cells. So far, we did not detect angiopoietin-1 in HT1080 cells, suggesting that other factors may mediate RECK induction. Several previous reports indicated candidates of mediator such as TIMP-1 or TGF-β (32, 33). However, we so far obtained no evidence that these soluble factors could affect RECK expression particularly in HUVECs (data not shown). Thus, we are currently examining other possible factors controlling RECK expressing in non-cell autonomous manner.

Taken together, our results indicate that tumor propagation via enhanced angiogenesis depends on the expression of RECK in proliferating vascular endothelial cells. We thereby propose that targeting RECK expressed in tumor vascular endothelial cells could be an interesting approach aiming to induce tumor regression.

Disclosure of potential conflicts of interest

No potential conflicts of interest were disclosed.

Acknowledgment

Grant support: Research Grant of the Princess Takamatsu Cancer Research Fund (05-23706), Takeda Science Foundation, and Japan Ministry of Education, Culture, Sports,

Science and Technology.

We thank M. Okabe for reagents, A. Nishimoto and H. Gu for technical assistance, and A. Miyazaki and M. Suzuki for secretarial assistance.

References

1. Nagase H, Woessner JF Jr. Matrix metalloproteinases. *J Biol Chem* 1999;**274**:21491-21494.

2. Egeblad M, Werb Z . New functions for the matrix metalloproteinases in cancer progression. *Nat Rev Cancer* 2002;**2**:161-174.

3. Visse R, Nagase H . Matrix metalloproteinases and tissue inhibitors of metalloproteinases: structure, function, and biochemistry. *Circ Res* 2003;**92**:827-839.

4. Jodele S, Blavier L, Yoon JM, DeClerck YA . Modifying the soil to affect the seed: role of stromal-derived matrix metalloproteinases in cancer progression. *Cancer Metastasis Rev* 2006;**25**:35-43.

5. Rundhaug JE . Matrix metalloproteinases and angiogenesis. *J Cell Mol Med* 2005;**9**:267-285.

6. Hynes RO . Cell-matrix adhesion in vascular development. *J Thromb Haemost* 2007;**1**:32-40.

7. Brooks PC, Silletti S, von Schalscha, TL, Friedlander M, Cheresh, DA . Disruption of angiogenesis by PEX, a noncatalytic metalloproteinase fragment with integrin binding activity. *Cell* 1998;**92**:391-400.

8. van Nimwegen MJ, van de Water B . Focal adhesion kinase: a potential target in cancer therapy. *Biochem Pharmacol* 2007;**73**:597-609.

9. Takahashi C, Sheng Z, Horan TP, et al . Regulation of matrix metalloproteinase-9 and inhibition of tumor invasion by the membrane-anchored glycoprotein RECK. *Proc Natl Acad Sci U S A*1998;**95**:13221-13226.

10. Liu LT, Peng JP, Chang HC, Hung WC . RECK is a target of Epstein-Barr virus latent membrane protein 1. *Oncogene* 2003;**22**:8263-8270.

11. Liu LT, Chang HC, Chiang LC, Hung WC . Histone deacetylase inhibitor up-regulates RECK to inhibit MMP-2 activation and cancer cell invasion. *Cancer Res* 2003;**63**:3069-3072.

12. Hu SJ, Ren G, Liu JL, et al . MicroRNA expression and regulation in mouse uterus

during embryo implantation. *J Biol Chem* 2008;**283**:23473-23484.

13. Gabriely G, Wurdinger T, Kesari S, et al . MicroRNA 21 promotes glioma invasion by targeting matrix metalloproteinase regulators. *Mol Cell Biol* 2008;**28**:5369-5380.

14. Zhang Z, Li Z, Gao C, et al . miR-21 plays a pivotal role in gastric cancer pathogenesis and progression. *Lab Invest* 2008;**88**:1358-1366.

15. Oh J, Takahashi R, Kondo S, et al . The membrane-anchored MMP inhibitor RECK is a key regulator of extracellular matrix integrity and angiogenesis. *Cell* 2001;**107**:789-800.

16. Miki T, Takegami Y, Okawa K, Muraguchi T, Noda M, Takahashi C . The reversion-inducing cysteine-rich protein with Kazal motifs (RECK) interacts with membrane type 1 matrix metalloproteinase and CD13/aminopeptidase N and modulates their endocytic pathways. *J Biol Chem* 2007;**282**:12341-12352.

17. Muraguchi T, Takegami Y, Ohtsuka T, et al . RECK modulates Notch signaling during cortical neurogenesis by regulating ADAM10 activity. *Nat Neurosci* 2007;**10**: 838-845.

18. Baker AH, Edwards DR, Murphy G . Metalloproteinase inhibitors: biological actions and therapeutic opportunities. *J Cell Sci* 2002;**115**:3719-3727.

19. Wayner EA, Gil SG, Murphy GF, Wilke MS, Carter WG . Epiligrin, a component of

epithelial basement membranes, is an adhesive ligand for alpha 3 beta 1 positive T lymphocytes. *J Cell Biol* 1993;**121**:1141-1152.

20. Okabe M, Ikawa M, Kominami K, Nakanishi T, Nishimune Y . 'Green mice' as a source of ubiquitous green cells. *FEBS Lett* 1997;**407**:313-319.

21. Shamma A, Takegami Y, Miki T, et al . Rb Regulates DNA damage response and cellular senescence through E2F-dependent suppression of N-ras isoprenylation. *Cancer Cell* 2009;**15**:255-269.

22. Sasahara RM, Takahashi C, Noda M . Involvement of the Sp1 site in ras-mediated downregulation of the RECK metastasis suppressor gene. *Biochem Biophys Res Commun* 1999;**264**:668-675.

23. Takahashi C, Bronson RT, Socolovsky M, et al . Rb and N-ras function together to control differentiation in the mouse. *Mol Cell Biol* 2003;**23**:5256-5268.

24. Nor JE, Peters MC, Christensen JB, et al . Engineering and characterization of functional human microvessels in immunodeficient mice. *Lab Invest* 2001;**81**:453-463.

25. Bryant P, Zheng Q, Pumiglia K . Focal adhesion kinase controls cellular levels of p27/Kip1 and p21/Cip1 through Skp2-dependent and -independent mechanisms. *Mol Cell Biol* 2006;**26**:4201-4213.

26. Menon B, Singh M, Ross RS, Johnson JN, Singh K . beta-Adrenergic receptor-stimulated apoptosis in adult cardiac myocytes involves MMP-2-mediated disruption of beta1 integrin signaling and mitochondrial pathway. *Am J Physiol Cell Physiol* 2006;**290**:254-261.

27. Jin EJ, Choi YA, Kyun Park E, Bang OS, Kang SS . MMP-2 functions as a negative regulator of chondrogenic cell condensation via down-regulation of the FAK-integrin beta1 interaction. *Dev Biol* 2007;**308**:474-484.

28. Devy L, Huang L, Naa L, et al. Selective inhibition of matrix metalloproteinase- 14 blocks tumor growth, invasion, and angiogenesis. *Cancer Res*. 2009;**69**:1517-1526.

29. Itoh Y, Seiki M. MT1-MMP: a potent modifier of pericellular microenvironment. *J Cell Physiol.* 2006;**206**:1-8.

30. Noda M, Takahashi C. Recklessness as a hallmark of aggressive cancer. *Cancer Sci.* 2007;**98**:1659-65.

31. Clark JC, Thomas DM, Choong PF. Et al. RECK--a newly discovered inhibitor of metastasis with prognostic significance in multiple forms of cancer. *Cancer Metastasis Rev.* 2007;**26**:675-83.

32. Lee H, Lim C, Lee J. et al. TGF-beta signaling preserves RECK expression in activated pancreatic stellate cells. *J Cell Biochem.* 2008;**104**:1065-74.

33. Oh J, Diaz T, Wei B. et al. TIMP-2 upregulates RECK expression via dephosphorylation of paxillin tyrosine residues 31 and 118. *Oncogene.* 2006;**25**:4230-4.

Figure legends

Figure 1. Roles of RECK in vascular development. A, HUVECs grown in the growth factor-free culture medium (EBM-2) and then treated with the indicated concentration of Angiopoietin-1 or other growth factors (10ng/ml) were analyzed by immunoblotting (IB) for the indicated proteins. NT: no treatment. **B**, Vascular phenotypes in mice of the indicated genotype at E10.0. Scale bar: 10 μm. Arrow: an endothelial cell detached from the subendothelial layer. **C**, HUVECs transfected with the indicated siRNA and grown in the culture medium supplemented with growth factors (EGM-2) were analyzed by IB (left). Two independent clones of siRNA targeting RECK (clone#1 and #2) were used. Endopeptidase activities to cleave Mca-Lys-Pro-Leu-Gly-DPA-Ala-Arg-NH_2 in the culture supernatants were measured (middle). Active per total MMP-2 was determined by precipitation with gelatin beads and following immunoblotting using antibody to MMP-2 (right). Bars are means + standard error (SE) from 3 experiments. **D**, The RT-PCR analysis of HUVECs transfected with the indicated siRNA, trypsinized, suspended for 30 min, replated on Matrigel, and grown for the indicated period of time (top). Cells at 48 h

were analyzed using light microscopy (bottom). Scale bar: 100 μm.

Figure 2. Effect of RECK depletion on the growth of HUVECs. A, Growth curve of HUVECs transfected with the indicated siRNA. Culture medium: EGM-2. Plots are means ± SE from 3 experiments. **B**, Cell cycle analysis of HUVECs at 48 h after transfection of the indicated siRNA. Data were obtained by FACS analysis. **C**, BrdU incorporation by HUVECs at 48 h after transfection of the indicated siRNA. Bars are means + SE from 3 experiments. **D**, Detection of SA-β-gal activity in HUVECs at 12 days after transfection of the indicated siRNA.

Figure 3. Effect of RECK depletion on HUVECs partially depends on MMP-2. A, Expression of the indicated proteins in HUVECs transfected with the indicated siRNA was analyzed by IB. Culture medium: EGM-2. **B**, Proliferation activity of HUVECs transfected with the indicated siRNA. Bars are means + SE from 5 experiments. **C**, HUVECs transfected with the indicated siRNA were grown on Matrigel for 48 h, and observed under light microscopy. Scale bars: 100 μm. **D**, Tube length and number of branches were measured. Control siRNA transfected HUVECs were set to 100. Bars are means + SE from 5 experiments. *, P value < 0.01.

Figure 4. The β1-integrin-dependent function of RECK. A, The activity of β1-integrin signaling in HUVECs transfected with the indicated siRNA was measured by FACS using the monoclonal antibody (9EG7) that specifically recognizes active form β1-integrin on the cell surface (top). Culture medium: EGM-2. The FACS result obtained

without adding the primary antibody is also indicated. The quantification of active (bottom left) and total (bottom right) β1-integrin is shown. The signal in cells transduced with the control siRNA was set to 1.0. Bars are mean + SE from 5 experiments. * P value < 0.01. **B**, HT1080 cells transfected with pCXN2-neo (Vector) or pCXN2-neo-RECK and selected were analyzed as in A. Bars are mean + SE from 3 experiments. **C**, The activity of β1-integrin signaling in HUVECs transfected with the indicated combinations of siRNA was measured as in panel A. Bars are mean + SE from 3 experiments. *, P value < 0.01. **D**, The autophosphorylation status and total amount of FAK were analyzed. **E**, Proliferation of HUVECs transfected with the indicated siRNA cultured in the presence of indicated concentrations of antibodies (P4G11). Bars are mean + SE from 5 experiments. *, P value < 0.01. **F**, The expression of the indicated proteins in HUVECs treated with the indicated siRNAs and antibodies (2 μg/ml) was analyzed. **G**, The expression of the indicated proteins in HUVECs treated with the indicated combinations of siRNAs was analyzed.

Figure 5. *Reck*-deficiency downregulates β1-integrin signaling in mouse embryos. A, Representative results of immunofluorescence (IF) analysis for the indicated proteins in the aorta of the indicated genotype of mice at E10.0 are shown. Total-β1-integrin^{+}/active β1-integrin^{-} endothelial cells are indicated by arrows. Scale bar: 10 μm. **B**, The activity of β1-integrin signaling is quantified from observation of 3 embryos of each genotype by assessing the frequency of active per total β1-integrin signals. Bars are mean + SE. *, P value < 0.01.

Figure 6. RECK induction in vascular endothelial cells supports tumor growth. A, IF analysis of the host mouse-derived blood vessels developed in a tumor generated by subcutaneously introducing 1 x 10^6 HT1080 cells into a 4 week-old Balb-c nu/nu mouse. Antibodies to the indicated proteins were used. Arrows indicate $RECK^+/CD31^+$ endothelial cells. Scale bars: 20 μm. **B**, Induction of RECK in HUVECs cocultured with HT1080 cells. 5 x 10^4 HUVECs were cocultured with 2.5 (+), 5.0 (++) or 10 (+++) x 10^4 HT1080 cells for 24 h (upper, top). Culture medium: Dulbecco's Modified Eagle's medium supplemented with 10% fetal calf serum. Endogenous RECK expression in the same number of HT1080 cells is also examined (upper, bottom). Induction of RECK in 5 x 10^4 HUVECs cocultured with the indicated tumor cell lines (5 x 10^4) (lower, top). Endogenous RECK expression in the same number of tumor cells is also examined (lower, bottom). **C**, A section from a human neuroblastoma obtained by biopsy was stained with hematoxylin and eosin (HE) (top). Scale bar: 100 μm. RECK expression in a $CD31^+$ blood vessel found in the tumor mass was detected by IF (bottom). Scale bar: 10 μm. **D**, HT1080 cells and HUVECs were loaded into PLLA scaffolds and grown in SCID mice for 3 weeks. Sections of different parts of a tumor (marginal and center) were stained for the indicated proteins (top). $CD31^+/hCD34^-$ cells: arrow heads; $CD31^+/hCD34^+$ cells: arrows. HT1080 cells and HUVECs transfected with the indicated siRNA were loaded into PLLA scaffolds and grown in SCID mice for 3 weeks. Tumor sections were stained for the indicated protein and DAPI (4',6-diamino-2-phenylindole) or by HE (bottom). Scale bar: 100 μm. Density of $hCD34^+$ endothelial cells (per x 40 magnification field, 10 fields were observed) (right, top) and tumor weights (right,

bottom) were measured. Bars are means + SE from 5 independent tumors. *, P value < 0.01; *, P value < 0.05.

Miki et al., Figure 1

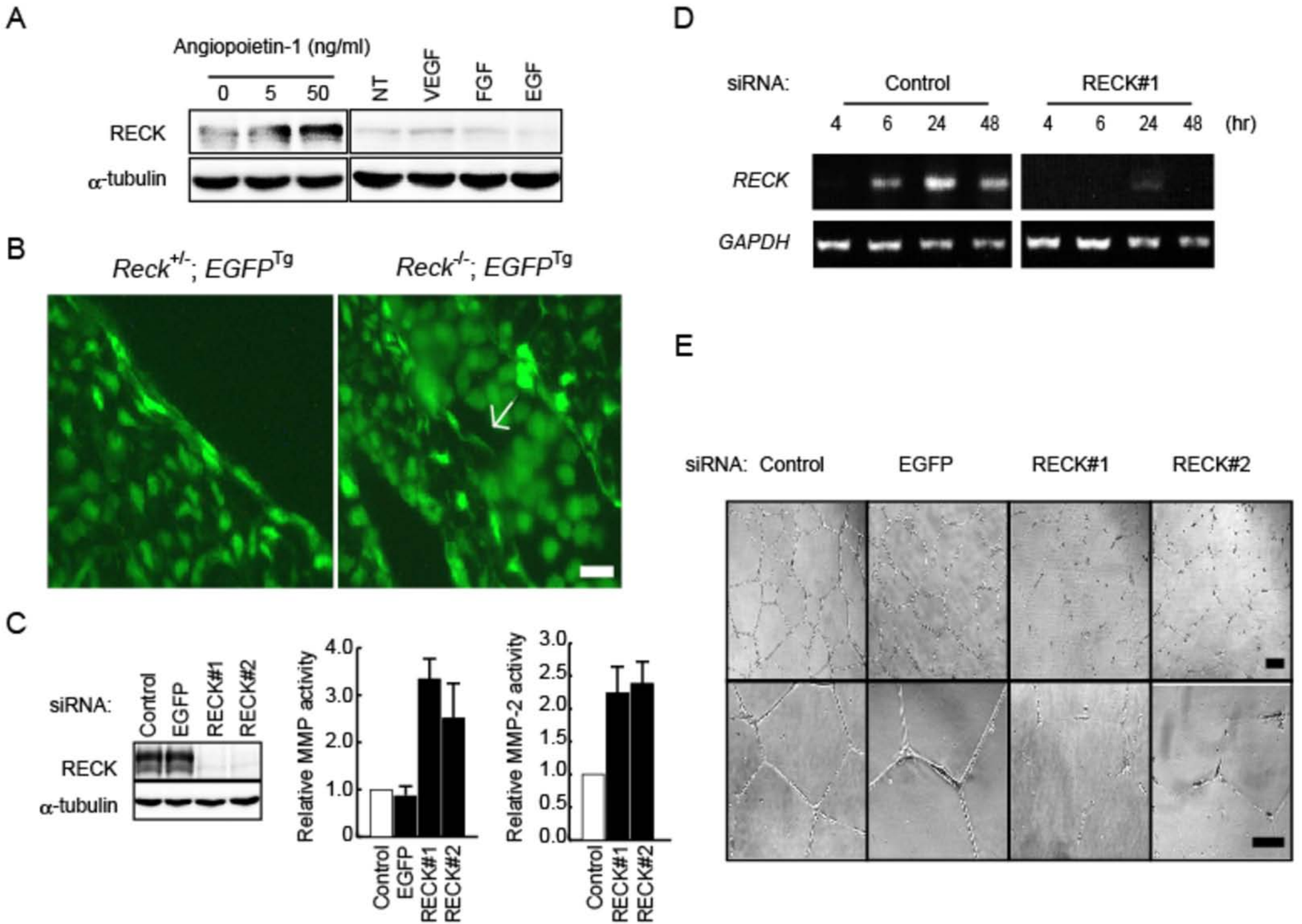

Miki et al., Figure 2

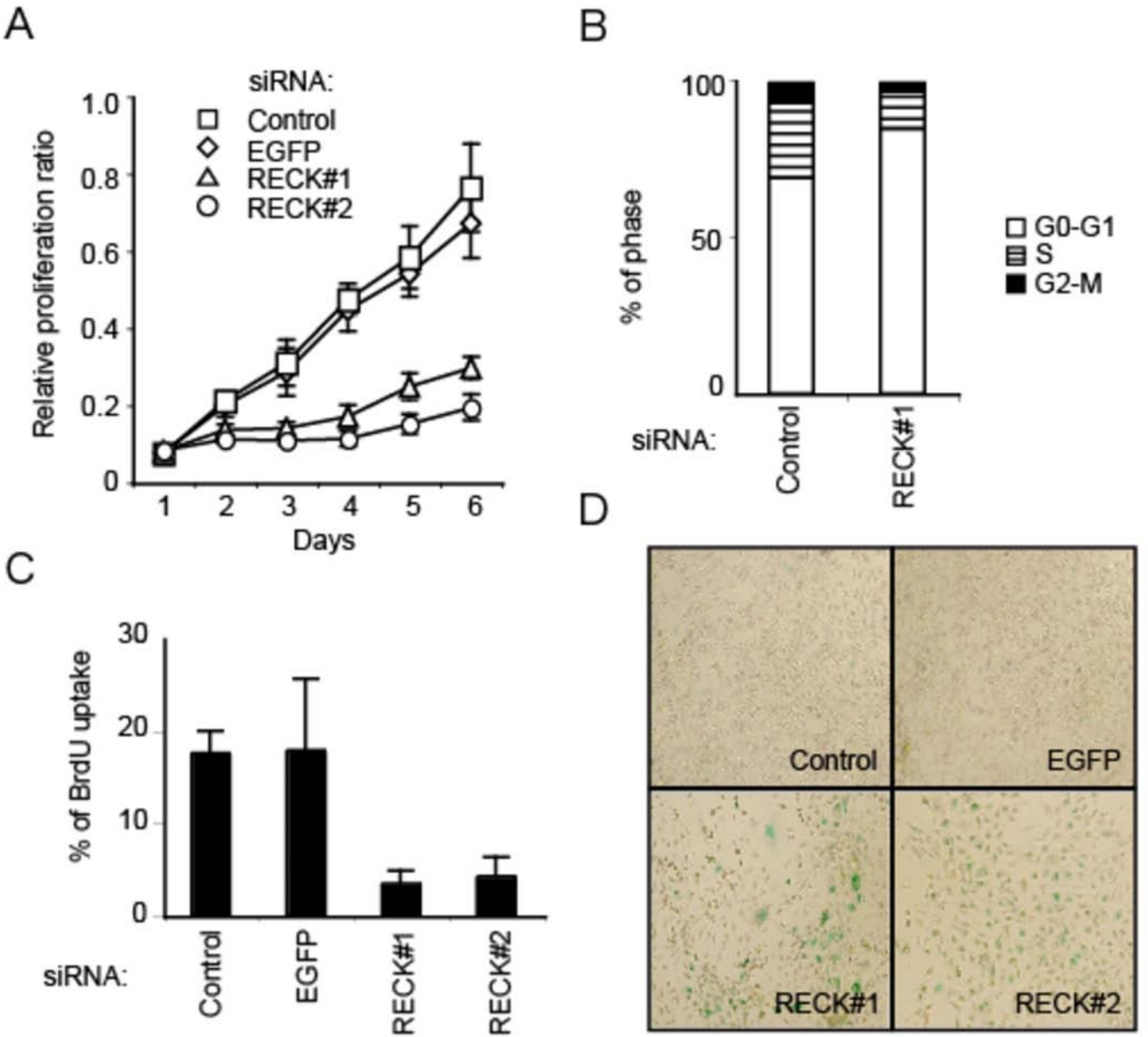

Miki et al., Figure 3

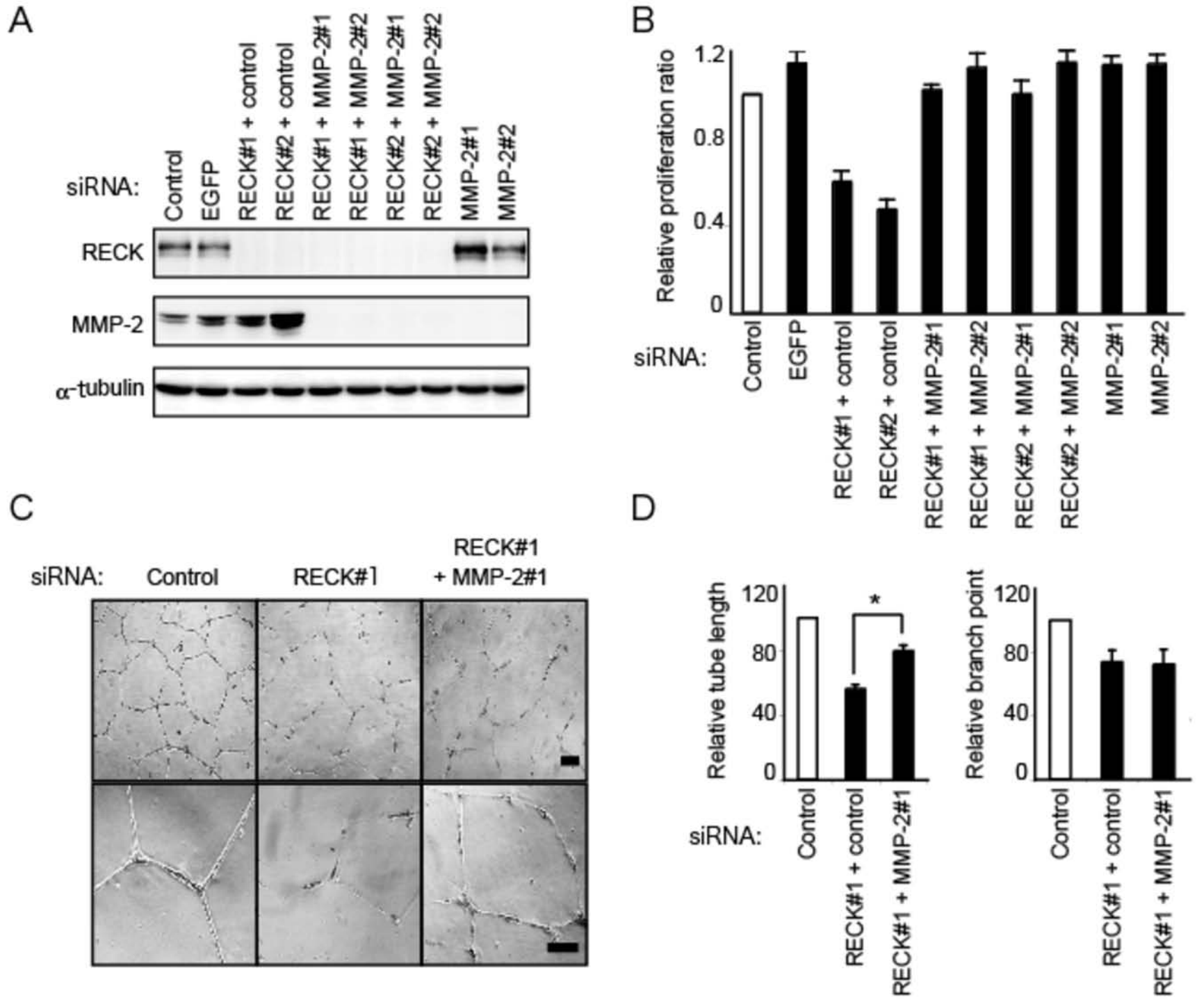

Miki et al., Figure 4

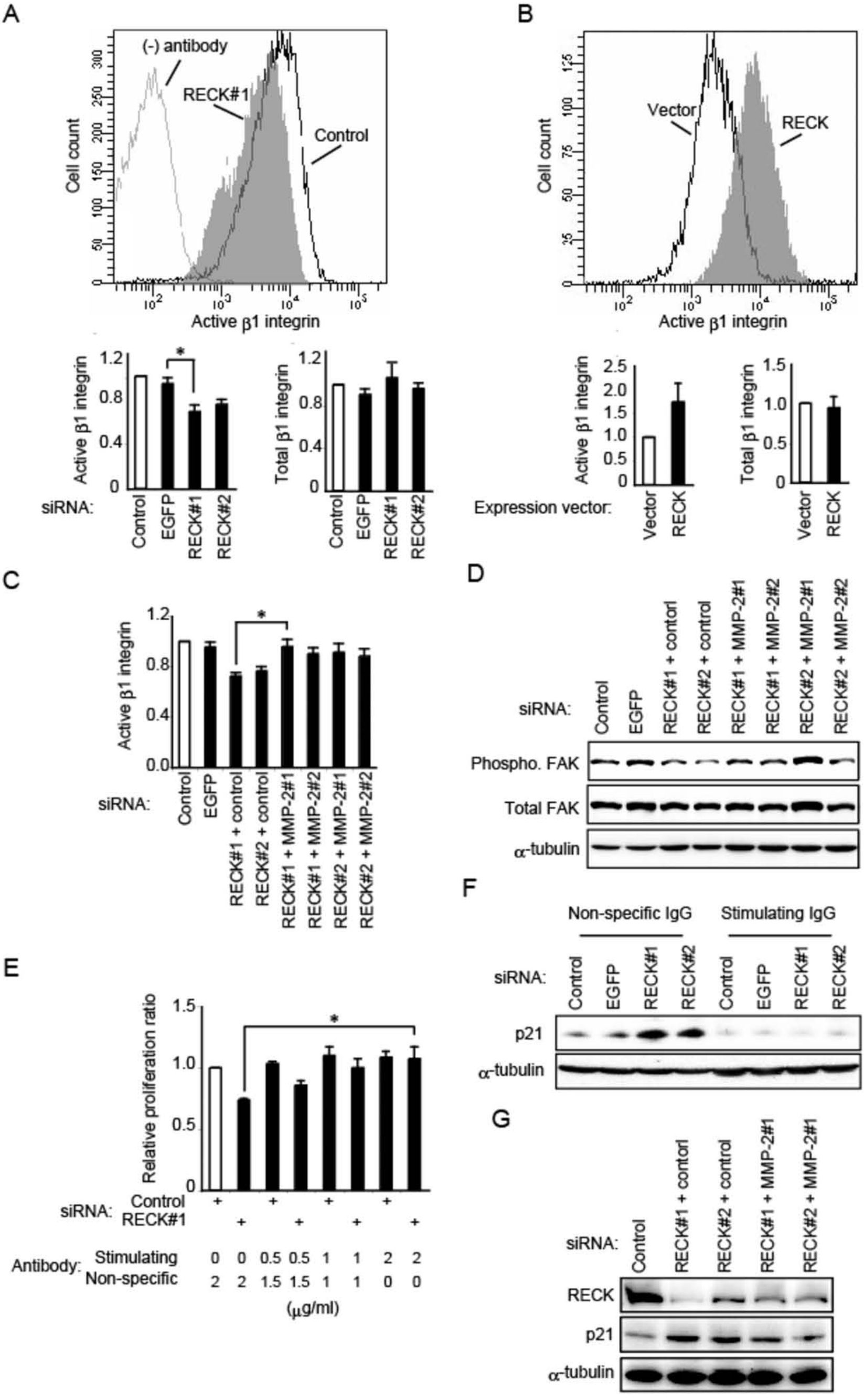

Miki et al., Figure 5

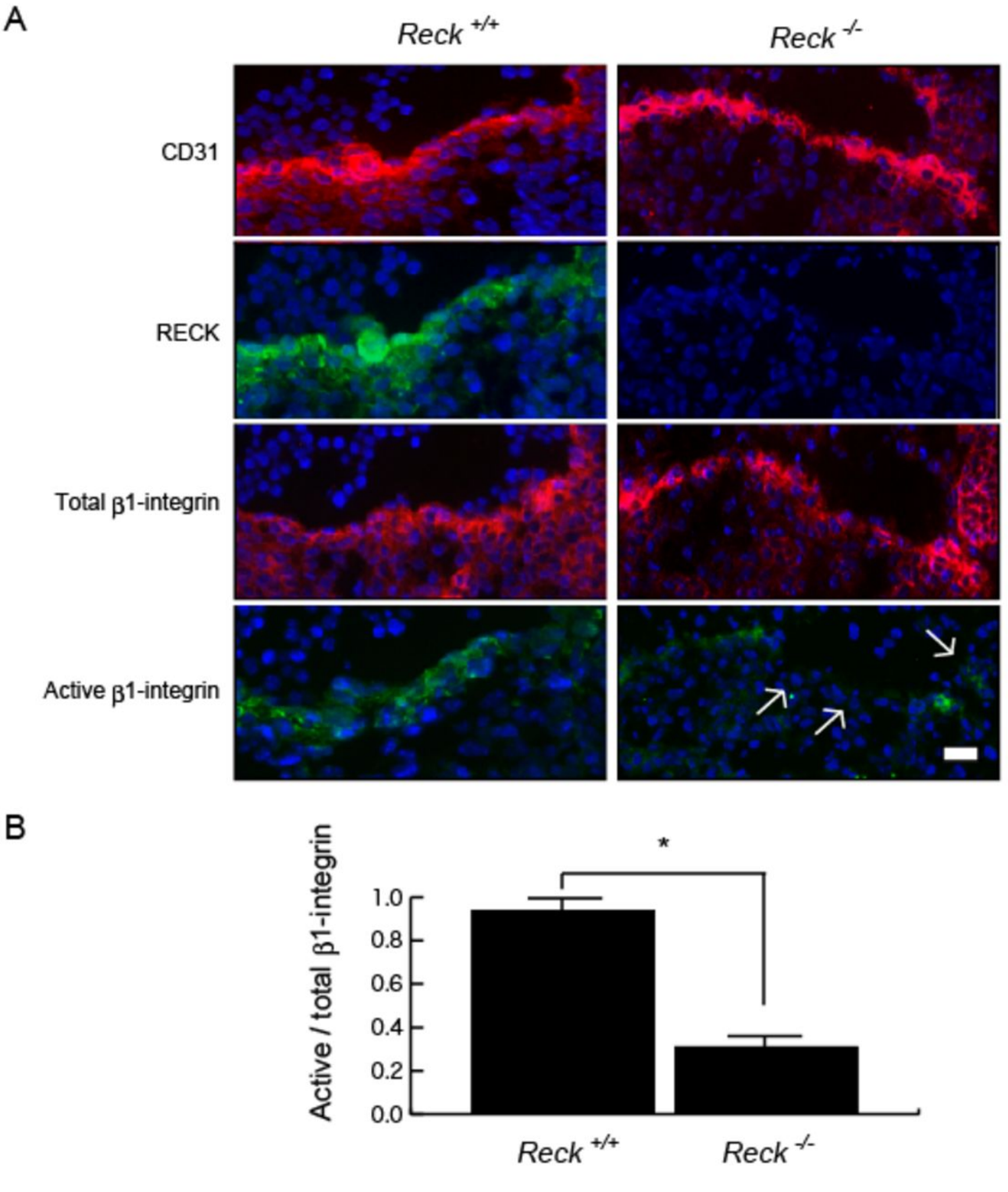

Miki et al., Figure 6